1996A&A...316..248M

Astron. Astrophys.316, 248–262 (1996)

ASTRONOMY AND ASTROPHYSICS

Origin and evolution of the Vesta asteroid family

F. Marzari [1], A. Cellino [2], D.R. Davis [3], P. Farinella [4], V. Zappalà [2], and V. Vanzani [1]

[1] Dipartimento di Fisica, Università di Padova, Via Marzolo 8, I-35131 Padova, Italy
[2] Ossevatorio Astronomico di Torino, I-10025 Pino Torinese, Italy
[3] Planetary Science Institute/SJI, 620 N. Sixth Avenue, Tucson, Arizona 85705-8331, USA
[4] Gruppo di Meccanica Spaziale, Dipartimento di Matematica, Università di Pisa, Via Buonarroti 2, I-56127 Pisa, Italy

Received 11 May 1995 / Accepted 13 March 1996

Abstract. We model the formation and subsequent collisional evolution of the Vesta asteroid family. The outcomes of the cratering event(s) which generated the family are predicted from current cratering physics, whereas the subsequent erosion of the family members due to collisions with background asteroids is simulated according to the model of Marzari et al. (1995). Comparing the size and orbital distribution of the model Vesta families with the observed family, we estimate the number and size of the projectile(s) which have impacted Vesta. The observed morphology of the family suggests two possible scenarios: (1) The family is the outcome of a major cratering event, resulting from the impact of an asteroid $\approx$ 40 km in diameter on the surface of Vesta about 1 Gyr ago, and followed by another more recent lower–energy impact (by a projectile $\approx$ 20 km in diameter), producing the family's subgrouping close to the 3:1 mean motion Jovian resonance. (2) A single impact occurred $\approx$ 1 Gyr ago and formed the whole family at the same time. In this case we have to assume that the fragments were ejected isotropically over a hemispheric region of Vesta, instead of being concentrated near the surface of a 90° aperture cone, as suggested by laboratory impact experiments with planar targets. This different ejection geometry yields a more scattered distribution of the orbital elements, resulting into a better agreement with the observed family. In both scenarios the cratering event(s) which formed the family is/are likely to have injected a significant number of km–sized and smaller fragments into the 3:1 resonance, thus generating V–type near–Earth asteroids and HED meteorites. However, it appears likely that the current influx of HED meteorites cannot be directly traced back to the family–forming event(s), but results from more recent, smaller impacts on Vesta (or other family members).

Key words: celestial mechanics – methods: numerical – minor planets, asteroids – meteors, meteoroids

Send offprint requests to: F. Marzari

1. Introduction

The first evidence that a large impact occurred on the asteroid (4) Vesta and ejected a spray of fragments into nearby space was the discovery of spectral similarity between the surface of this asteroid and the howardite/eucrite/diogenite (HED) basaltic achondrite meteorites. McCord et al. (1970) measured the reflectance spectrum of Vesta with moderate spectral resolution and identified a deep absorption band at a wavelength of about 0.9 μm, which they interpreted as diagnostic of the mineral pyroxene. They proposed that the surface material of the asteroid was similar to the HED meteorites. This spectral relationship suggested that Vesta might be the parent body of these meteorites (see e.g. Drake 1979; Greenberg & Chapman 1983). More recently, Cruikshank et al. (1991) have found that three km–sized near–Earth asteroids (NEAs) display basaltic reflectance spectra nearly identical to that of Vesta; hence, they have been classified as V–types, a taxonomic class whose only main–belt member larger than 15 km in diameter is Vesta itself. This kind of data supports the idea that fragments from Vesta can be inserted into Earth–crossing orbits. The main difficulty with this possibility has always been the high ejection velocity — at least some 600 m/s — needed to reach a resonant zone of the orbital element space starting from Vesta; this also led Wetherill (1987) to the conclusion that the Earth–impact efficiency for Vesta's ejecta must be very low.

However, there is independent evidence supporting the idea that high–velocity fragments have been ejected from Vesta. In his table of asteroid proper elements and family memberships, Williams (1979; see also his 1989 and 1992 papers) for the first time proposed the existence of a Vesta family (family 169). He identified the family by looking at the distribution of proper elements in a sample of 1753 numbered and 1070 unnumbered (PLS) asteroids, and noting that seven small asteroids (only one numbered) were fairly close to Vesta in proper element space. He suggested that the small family members might be interpreted as ejecta from a cratering event on Vesta.

More recently Zappalà et al. (1990, 1994) performed a new search for families based on a much larger sample of asteroids than Williams had used. In the 1994 work, they used 6,212 ob-

© European Southern Observatory • Provided by the NASA Astrophysics Data System

1996A&A...316..248M

jects, about 70% numbered, whose proper elements had been derived by Milani & Knežević (1992). Using the hierarchical clustering method, an automated computer algorithm well suited for identifying families, they found an extensive Vesta family consisting of 64 objects between about 2 and 10 km in size. This finding has led to the testable prediction that the small Vesta family members should be spectrally similar to Vesta: a prediction readily confirmed by a spectroscopic survey carried out by Binzel & Xu (1993), who observed a number of these objects as well as many other small asteroids lying in the same region of proper element space, and found a remarkable spectral similarity between Vesta and several members of the family. Thus Vesta is not any longer the only main–belt asteroid displaying a spectrum similar to those of HED meteorites, and a number of minor Vesta family members can also be assigned to its peculiar (V) taxonomic type. This clearly confirms the genetic relationship between them and Vesta. The relationship with the achondrite meteorites, on the other hand, is supported by Binzel's and Xu's finding that eight small Vesta–like asteroids are located between Vesta and the 3:1 Jovian mean motion resonance, an effective delivery *route* from the main belt for both meteorites and near–Earth asteroids (Wisdom 1983, 1985; Yoshikawa 1990; Moons & Morbidelli 1995). Actually, Binzel & Xu also noted that among the Vesta–like small asteroids, spectral features more analogous either to the eucrite or to the diogenite classes of basaltic achondrites are found.

In the latest family search by Zappalà et al. (1995, with a 12,487 asteroid sample) the Vesta family membership has increased to more than 200 (see Sect. 2). The large gap in size between Vesta and the other family members strongly suggests that the Vesta family was generated by an energetic impact cratering event, ejecting a large number of fragments from Vesta's surface at speeds exceeding $\approx$ 350 m/s (Vesta's escape velocity). Although recent small scale experiments by Gratz et al. (1993) show that impacts can effectively eject small quantities of surface material at high velocities from a target surface, we are still far from a complete physical understanding of large cratering events and in particular of the size and velocity distributions of the ejecta. But we believe that the velocity problem, though deserving further scrutiny, cannot in itself rule out the reality of the Vesta family as a collisional outcome. As far as the meteorite connection is concerned, Farinella et al. (1993) have recently confirmed that the average ΔV of Vesta fragments reaching the 3:1 mean motion Jovian resonance is about 700 m/s (and exceeds 1 km/s for the ν_6 secular resonance). Despite this high velocity, they found that its large size can make Vesta a relatively efficient ejecta deliverer to the chaotic zones of the orbital element space.

Finally, relevant data on Vesta itself have been provided by physical observations of this asteroid. Gaffey (1983) revealed significant rotational variations in his spectra of Vesta. From the analysis of these data he reached the conclusion that the spectral variations are due to at least one large crater on the basaltic crust of Vesta, the product of a giant impact which exposed deeper strata on the asteroid surface. Eucrite and diogenite meteorites would be samples of Vesta's crustal material and of this deeper excavated layer, respectively. Gaffey's observations also implied that Vesta cannot have undergone a catastrophic collision converting it in a large rubble pile, and this provides a significant constraint on the intensity of the past collisional flux in the asteroid belt (Davis et al. 1985, 1994). A more recent reanalysis of the available spectrophotometric data (Gaffey 1996) has led to the tentative identification of a few distinct impact basins which penetrated Vesta's crust, concentrated in one hemisphere and possibly generated by comparatively recent ($< 10^9$ yr) collisional events. This is fully consistent with Vesta's hemispheric–scale photometric and polarimetric variations, as well as with speckle interferometry data (Cellino et al. 1987, 1989; Drummond et al. 1988; Lupishko et al. 1988; Broglia & Manara 1989). Recent images of Vesta obtained with the Hubble Space Telescope (Zellner et al. 1995) have confirmed the large–scale albedo and colour variegation of the surface.

We have adopted in this paper a numerical approach to model the cratering event(s) on Vesta and to simulate the subsequent evolution of the family due to catastrophic collisions with "background" asteroids (Marzari et al. 1995). The cratering events on Vesta have been modeled using laboratory experiment results, theoretical work on scaling algorithms and observational constraints from the Vesta family. We have also kept track in our model of the orbital distribution of the small fragments generated by the cratering impacts, in order to match the observed features of the family and to study the possible connection between Vesta's ejecta and the 3:1 resonance.

The remainder of this paper is organized as follows. The morphology of the Vesta family resulting from the latest family search by Zappalà et al. (1995) is described in Sect. 2. The cratering physics used in our model is discussed in Sect. 3. In Sects. 4 and 5 we analyse the constraints on the family's origin and evolution provided by the data on its size and orbital element distribution, respectively. Finally, in Sect. 6 we summarize our main results and discuss the remaining open problems.

2. Morphology of the Vesta family

For what concerns the number and identity of the Vesta family members, in the present paper we refer to the most recent results obtained by Zappalà et al. (1995). These authors have carried out a new search for asteroid families in the main belt, using both the modern automated methods of family identification developed in recent years, namely the *hierarchical clustering method* (HCM; Zappalà et al. 1990, 1994) and the *wavelet analysis method* (WAM; Bendjoya et al. 1991; Bendjoya 1993). These methods are independent, being based on different general principles, as explained in the above–mentioned papers. Moreover, their performances have been extensively and comparatively checked by means of suitable numerical simulations (Bendjoya et al. 1993) and have been found to be satisfactory even in extreme situations of small families plunged in a dense random background.

With respect to the previous searches, the main difference in the case of the Zappalà et al. (1995) work has been the size of the

© European Southern Observatory • Provided by the NASA Astrophysics Data System

1996A&A...316..248M

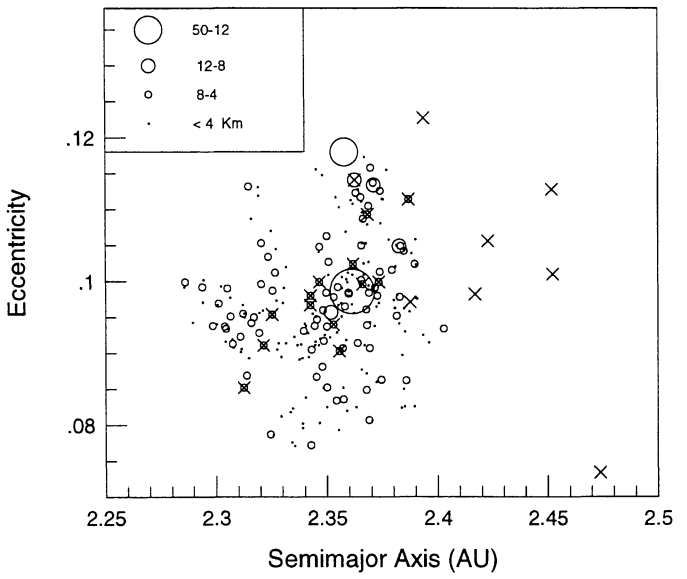

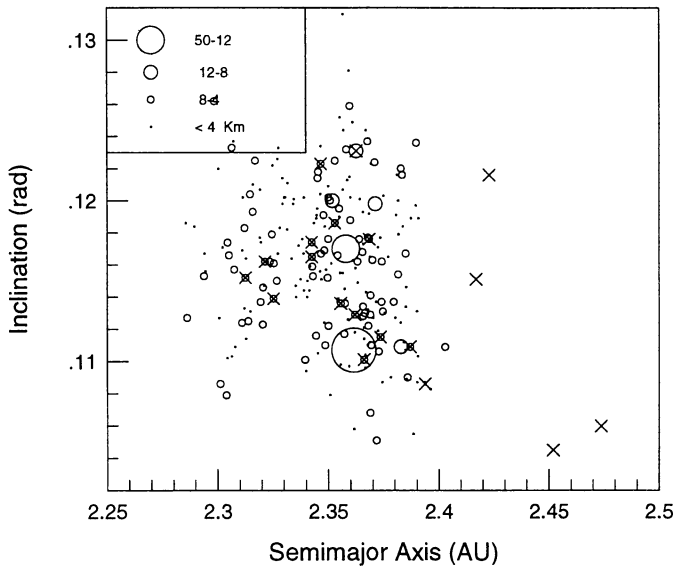

Fig. 1a and b. The distribution of Vesta family members identified by HCM at a distance level of 120 m/s in the proper semimajor axis vs. proper eccentricity **a** and proper semimajor axis vs. proper inclination **b** planes. Larger circles represent larger asteroids, as shown in the upper left corner of the figure. The locations of the 20 small objects found by Binzel & Xu (1993) to have spectra similar to that of Vesta is shown by crosses.

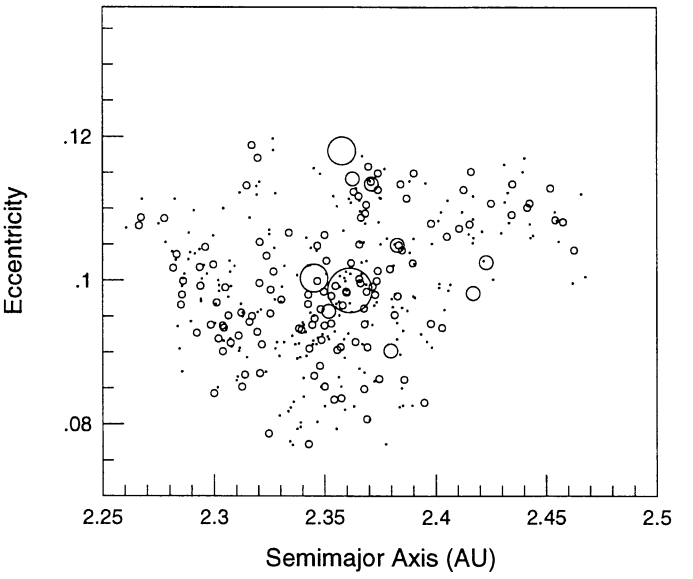

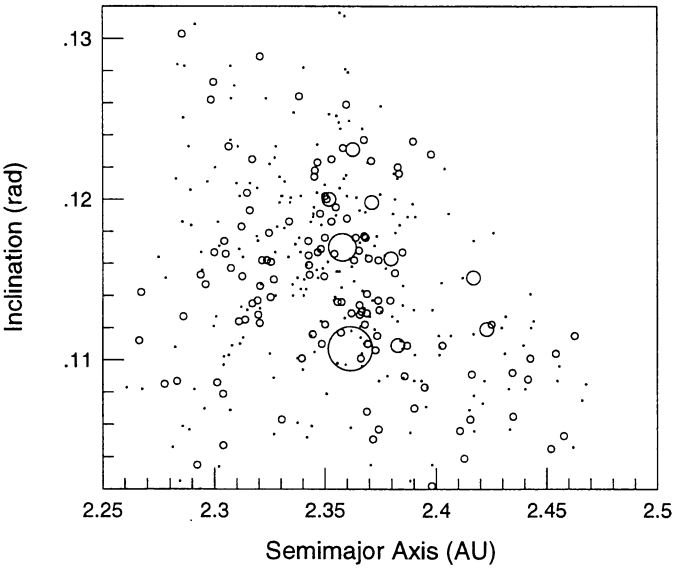

Fig. 2a and b. The same as Figs. 1a and b, but defining the family at a distance level of 140 m/s.

adopted data base of asteroid proper elements. The sample consisted of 12,487 main belt asteroids, including all the objects numbered up to the beginning of 1993 (about 4600 objects), plus about 2200 unnumbered asteroids observed at more than one opposition, as well as about 5800 unnumbered objects observed at one opposition only, but having osculating elements of a sufficiently good quality for a reliable computation of proper elements (Milani et al. 1994). This data set is about twice as large with respect to the one previously used by Zappalà et al. (1994) and Bendjoya (1993).

In the case of the Vesta family, the results obtained by Zappalà et al. (1995) using either HCM or WAM show fairly good agreement. The family is clearly recognized by both methods, and actually looks like one of the most prominent groupings located in the inner region of the main belt. The nominal members found by the two techniques are 231 (HCM) and 242 (WAM), with 187 objects being identified as family members by both techniques. This means that 81% of the nominal family members found by HCM are confirmed by WAM, whereas 77% of the members found by WAM are confirmed by the HCM results. As explained by Zappalà et al. (Sect. 5), the differences are due in part to a different response of the two techniques to the features of the asteroidal distribution in proper element space. Also, defining unequivocally the membership of the family is difficult because it has the structure of a typical *clan*, follow-

© European Southern Observatory • Provided by the NASA Astrophysics Data System

1996A&A...316..248M

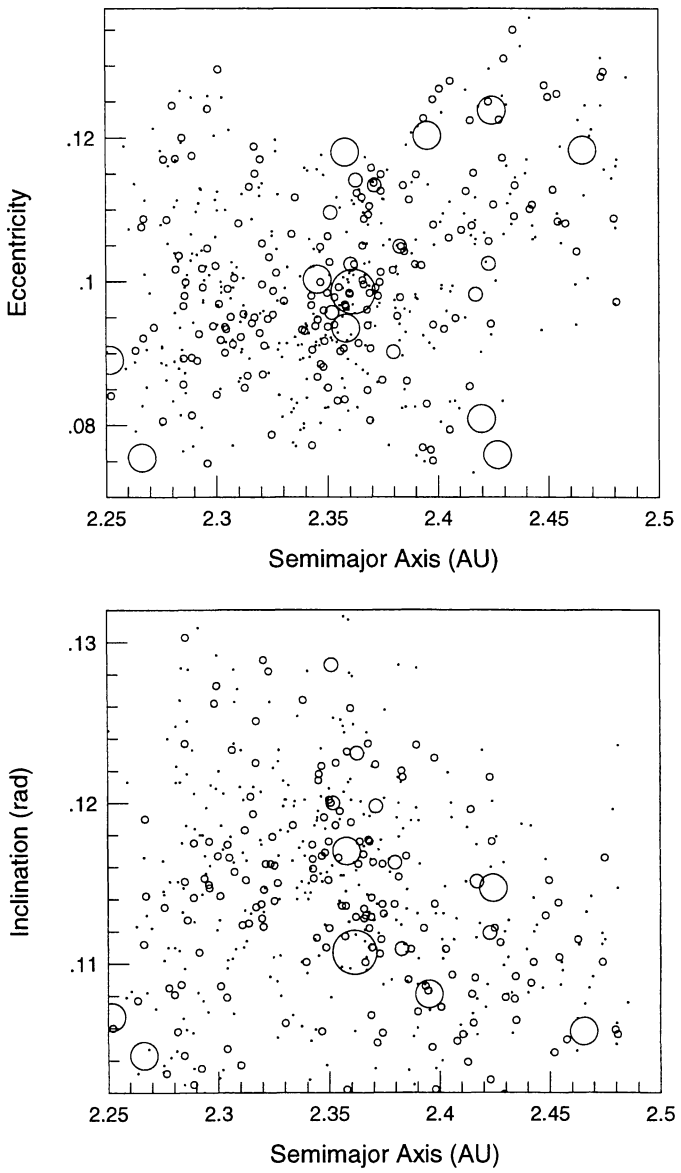

Fig. 3a and b. The same as Figs. 1a and b, but defining the family at a distance level of 170 m/s.

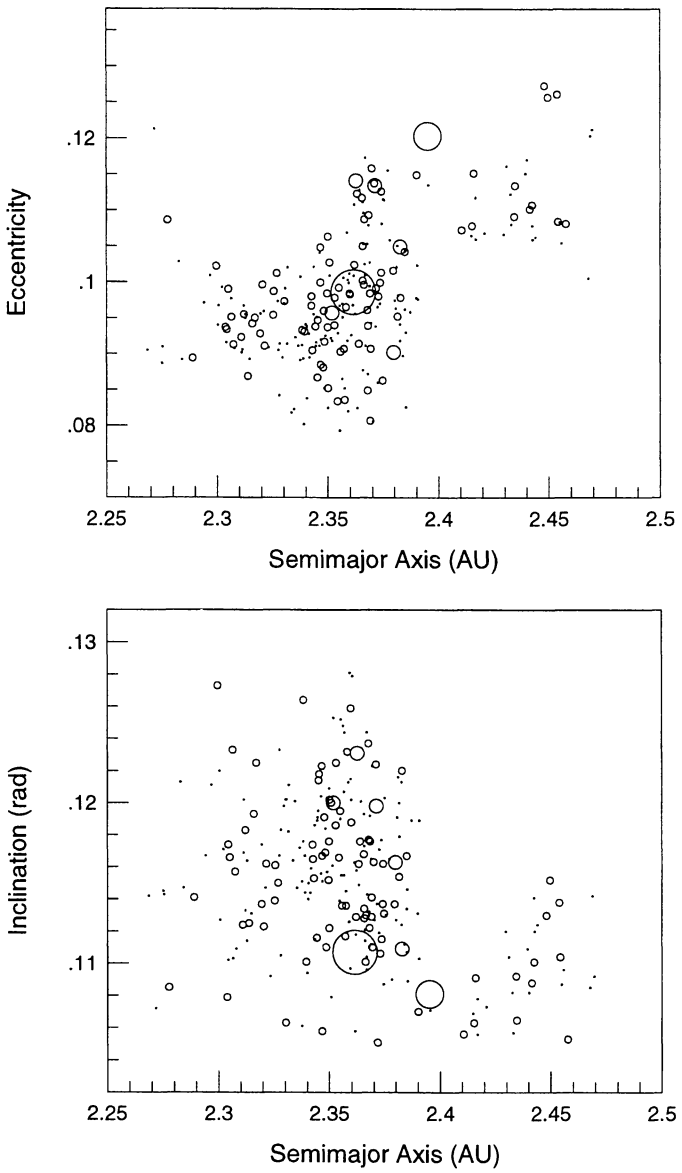

Fig. 4a and b. The same as Fig. 1, but for the family membership identified by WAM.

ing the nomenclature introduced by Farinella et al. (1992). This can be best understood by looking at the *stalactite diagrams* that are the output of the HCM technique, and show how much a given grouping is compact and sharply defined with respect to the background, as a function of the maximum allowable "distance" between its members in proper element space (Farinella et al. 1992; Cellino & Zappalà 1993; Zappalà & Cellino, 1992, 1994). In particular, clans are groupings with fairly uncertain borders and a complex internal structure. Therefore, their membership depends strongly upon the adopted distance threshold (or any other rejection criteria).

In the case of Vesta, the reader should refer to the stalactite diagram of the inner zone of the asteroid belt shown in Fig. 6 of the Zappalà et al. (1995) paper. The nominal membership of the family obtained by HCM was defined at a distance level of 120 m/s. However, we recall that distances in proper element space can be expressed as velocities, as they are computed from the change of orbital elements caused by a given velocity increment δV (see, e.g., Milani et al. 1992). Thus, higher distance levels correspond to "looser" groupings, consisting of asteroids separated by δV's up to a higher upper limit, and *vice versa*. Just because we deal with a *clan*, the nominal membership should be considered with care. In such cases, Zappalà et al. remark that often the HCM criteria happen to be somewhat conservative. Therefore, we have analyzed the structure of the family also at different distance levels, i.e., by "cutting the stalactite" at higher velocity values. This allows us to detect possible changes in the structure of the family in proper element space, looking at the same time for the best agreement with respect to the family membership found by WAM.

© European Southern Observatory • Provided by the NASA Astrophysics Data System

1996A&A...316..248M

The structure of the Vesta family as found by HCM at different distance levels (120, 140 and 170 m/s, respectively) is shown in Figs. 1 to 3, where the family members are plotted with progressively larger circles for increasing diameters. The IRAS data base (Tedesco 1994) has been used to derive the sizes of some family members, while for the objects not observed by IRAS the diameter has been calculated from their H magnitude assuming an albedo of 0.3. This is a typical value for V–type asteroids, taking into account also the Apollo–Amor V–type objects (Cruikshank et al. . 1991). In the same plots, the position of Vesta is shown by the largest circle. In Fig. 1, we also show the locations of the objects spectrally similar to Vesta identified by Binzel & Xu (1993). These figures can now be compared with the corresponding ones (Figs. 4a,b) showing the structure of the family as found by WAM.

The comparison shows that the main difference between the nominal HCM results (i.e., the members found at the 120 m/s distance level, see Figs. 1) and the WAM results is the lack in the HCM family of a subgrouping located at semimajor axis values larger than Vesta, and fairly close to the inner edge of the 3:1 Kirkwood gap. This feature is instead clearly recognizable in the HCM plots referring to the distance value of 140 m/s (Figs. 2) and, of course, 170 m/s (Figs. 3), although in the latter case the family also includes a large number of other objects, among which there are probably many chance interlopers, i.e. objects with no genetic relationship to Vesta.

The importance of the subgrouping close to the 3:1 resonance is due to its implications concerning the possible injection of fragments into this resonance. The fact that objects spectrally similar to Vesta have been discovered in this region (see Figs. 1) suggests that it is actually populated by many small family members, namely fragments ejected at high velocities toward the resonance. From this point of view, the nominal membership of the family found by HCM at 120 m/s is certainly conservative, and the real family is probably much better represented by the membership found at 140 m/s. This would also lead to a better agreement between the HCM and WAM results (compare Figs. 2 and 4). Also, the overall structure of the family shows that Vesta is located at a somewhat peripheric location in it (this is apparent in the projection on the semimajor axis vs. inclination plane). This morphology is not consistent with the isotropic ejection of fragments from Vesta, but rather with an anisotropic ejection mechanism. A plausible such mechanism is a very energetic cratering event, leading to the formation of a large–scale impact basin on one side of the asteroid. This interpretation is supported by the physical observations of Vesta summarized in Sect. 1. Of course, more complicated scenarios — e.g., involving more than one cratering impact — cannot be ruled out *a priori*, and the aim of this paper is just to assess in a semi–quantitative way the constraints provided by the observed properties of the family on the collisional history of Vesta.

Finally, we may wonder how many interlopers the family identified by the clustering techniques is likely to include. Migliorini et al. (1995) have recently dealt with this problem and have estimated the abundance of interlopers in all the nominal HCM families identified by Zappalà et al. (1995). Their method is based on estimating the volume of the family in proper element space and the density of background objects in the same zone of the asteroid belt, for different diameter ranges. In the case of the Vesta family, they concluded that: (1) the number of interlopers is likely to be fairly low, $\approx$ 10 up to 10 km in diameter and a few for larger sizes; (2) as expected, the nominal HCM family (defined at 120 m/s) is probably conservative, as the region of proper element space lying just around it contains a significantly higher number of objects than predicted from the overall background density. Along with the previous results on the comparison between the HCM and WAM results, the latter conclusion has led us to base our modeling effort on the membership and morphology of the HCM family at the 140 m/s (rather than 120 m/s) distance level. It is also interesting to note that physical data suggest that at least one sizeable nominal family member [(306) Unitas, with an IRAS diameter of about 47 km] is actually an interloper, since it is classified as an S–type asteroid in all the existing taxonomic classifications (Tholen 1989, Tedesco et al. 1989); therefore this object will not be included in the family's size distribution to be discussed later.

3. Modeling the cratering event

To model a cratering event on the surface of a large asteroid like Vesta (about 520 km in diameter, according to Dunham 1991) we adopt the scaling approach described in Holsapple (1993). We estimate the amount of mass excavated in the cratering process based on the "cratering efficiency" π_V, a dimensionless parameter defined as the ratio between the mass excavated from the crater M_{exc} and the mass m_p of the projectile. From Holsapple (1993), π_V can be expressed as a function of the dimensionless variable π_2, given by:

$$\pi_2 = \frac{gD_p}{2V_i^2}\,, \tag{1}$$

where g is the gravitational acceleration on the surface, D_p is the diameter of the projectile and V_i is the impact velocity. Note that for a crater of depth $\approx D_p$, the product $\pi_2\pi_V$ is just proportional to the ratio between the gravitational potential energy of the excavated mass and the projectile's kinetic energy, with a coefficient of order unity. We do not take into account in our model the dependence of π_V on the target material properties, because for sufficiently large impact events (craters of diameter exceeding $\approx$ 1 km in the case of Vesta) we are in the so–called "gravity regime" and the effects of gravity dominate over the effects of material strength (for a detailed discussion of scaling laws for crater dimensions, we refer to Melosh 1989, Ch. 7). In the gravity regime, the experimental relationship between π_V and π_2 found by Holsapple for rock is:

$$\pi_V = 0.095\pi_2^{-0.65}\,. \tag{2}$$

Given the projectile's size and the impact velocity, we use this relationship to estimate the amount of excavated mass.

To describe how the number of fragments varies with fragment mass we assume a single–exponent power–law distribution $N(>m) = Cm^{-b}$, in agreement with the results from

© European Southern Observatory • Provided by the NASA Astrophysics Data System

1996A&A...316..248M

laboratory–scale impact craters, nuclear explosion craters and ejecta from large terrestrial and lunar impact craters (see Melosh 1989, Ch. 6). To compute the exponent b and the normalizing constant C of the power law we follow three different alternative approaches:

1. Following several previous models for the outcomes of high–velocity impacts (e.g., Greenberg et al. 1978; Davis et al. 1989; Petit & Farinella 1993), we set the exponent b to 0.8. If the power law is extrapolated assuming that there is a single largest fragment of mass M_{LF}, then $C = M_{LF}^b$ and conservation of mass yields:

$$M_{LF} = \frac{(1-b)}{b} M_{exc} = \frac{M_{exc}}{4} . \quad (3)$$

   Hereafter we will refer to this approach as PF93.
2. According to Melosh (1989), we cut the size distribution of the fragments at the high mass end, assuming that the largest fragment is a function of the excavated mass M_{exc} through the relation:

$$M_{LF} = 0.8 \times M_{exc}^{0.8} , \quad (4)$$

   with masses expressed in kg. The coefficients b and C are then derived from the conservation of mass. Values of b very close to 1 (or even > 1, if a lower cutoff is assumed in the mass distribution) are implied for large craters, since according to Eq. 4 in this case $M_{LF} << M_{exc}$; therefore, a large amount of mass resides in small fragments. This approach will be named as M89.
3. In the third approach, the largest size for the ejected fragments is set by the thickness of Vesta's basaltic crust. This idea is consistent with Gratz's et al. (1993) experimental results on the ejection of fast fragments from the target's surface. The diameter cutoff we assume in our model is 25 km, corresponding to a crust accounting for $\approx$ 30% of Vesta's mass. This is reasonable on cosmochemical grounds (Gaffey et al. 1994). Also, Vesta's crust could not be thinner than the size of the observed minor family members, otherwise we would not observe a significant fraction of eucritic fragments; nor could it be more than $\approx$ 40 km in thickness, otherwise the diogenite fragments could not have been excavated from the bottom of a crater some 200 km across [according to Gaffey's (1996) estimate]. In this case, the coefficient b is set to 0.8 as in PF93, but whereas in that case (as well as in M89) the largest fragment was assumed to be a single body and its mass was used to compute C, in this approach multiple largest fragments of the same size (25 km in diameter) are assumed to have been ejected. Then the number of bodies as a function of size is computed from the power–law distribution. We will call this approach VBC.

In the next section we will compare results for the Vesta cratering event obtained from the application of the three different methods for computing the size distribution of the fragments as outlined above.

As for the mass–velocity distribution of the ejecta, we shall adopt the relationship

$$V(m) = V_0 \left(\frac{m}{M_{LF}} \right)^{-r} , \quad (5)$$

with M_{LF} the mass of the largest body and V_0 a constant which is found using the conservation of energy (a fraction f_{KE}^{cr} of the projectile's kinetic energy is assumed to be partitioned into kinetic energy of the ejecta). This equation is consistent with the concept that small fragments are ejected at higher velocities than large ones, in agreement with the results of small–scale impact experiments (e.g., Nakamura & Fujiwara 1991, Nakamura et al. 1992) and with the properties of the secondary craters surrounding some large impact craters on Mercury, the Moon and Mars (Vickery 1986, 1987). The exponent r is derived from:

$$r = \frac{(1-b)}{k} , \quad (6)$$

where $k = 9/4$ is the exponent of the cumulative mass vs. velocity distribution determined experimentally by Gault et al. (1963). Actually, Eq. 5 would predict a deterministic relationship between fragment mass and velocity, whereas both laboratory data and crater studies show that there is a considerable amount of dispersion around such a power–law fit. To simulate this dispersion, we superimpose to the deterministic relationship a statistical noise, as in Petit & Farinella (1993). A random velocity v is derived for each fragment of mass m from a Maxwellian distribution

$$P[v; V(m)]\, dv = \sqrt{\frac{2}{\pi}} \frac{3\sqrt{3}v^2}{V^3(m)} \exp\left[-\frac{3v^2}{2V^2(m)} \right] dv , \quad (7)$$

where $V(m)$ is the deterministic value derived by Eq. 5. For each fragment the ejection velocity is then compared to the escape velocity of the parent body (a density of 3 g/cm^3 is assumed for Vesta). Whenever v is lower than the escape velocity, the body is reaccumulated and its mass is added back to that of Vesta, otherwise the fragment is assumed to reach an independent heliocentric orbit.

The 3–D velocity field of the fragments has been computed by assuming a conical distribution of the velocity vectors around the perpendicular to the impact site, as suggested by most small–scale experiments performed in a vacuum (see Melosh 1989, Ch. 6). The impact site and the orientation of the ejecta cone axis with respect to the orbital plane of Vesta is determined by two angles: the polar angle Φ between the orbital plane and the cone axis, and the azimuthal angle Θ defined from the along–track direction of Vesta's orbit. As we shall see in Sect. 5, these parameters can be adjusted in order to obtain a better fit to the observed orbital distribution of the family. The opening angle of the ejecta cone α (defined as half its total aperture) is normally set to 45°, based on evidence from impact experiments into planar surfaces. However, we have reason to think that α may become larger in the case of giant craters on spherical surfaces. If the size of the crater is a significant fraction of the diameter of the target, then the curvature of the surface adds to the 45°

© European Southern Observatory • Provided by the NASA Astrophysics Data System

1996A&A...316..248M

zenith angle of the ejecta, if the latter is considered with respect to the perpendicular to the crater edges (and not to the crater's center). Thus, we will also consider as a limiting case an impact generating an ejecta cone whose opening angle with respect to the center of the target asteroid is 90°, corresponding to a 180° total aperture of the ejecta cone, i.e., to ejecta starting along a plane.

For a comparatively large target body like Vesta, we have also to take into account the deflection of the velocity vectors induced by the gravity field of the cratered object. Massive fragments are most affected by this phenomenon, owing to their small ejection velocity. Knowing the initial velocities and the ejection angles, we describe the ballistic trajectories of the fragments as hyperbolae and compute their final direction "at infinity" with respect to the parent body. For each fragment, we derive at the ejection time (i.e., at the parent's surface) a relationship between α_0, the initial angle between the axis of the cone and the ejection velocity, and f_0, the initial true anomaly along the hyperbolic orbit:

$$\cos f_0 = \frac{1}{e}\left(\frac{2V^2 sin^2\alpha_0}{V_e^2} - 1\right), \quad (8)$$

where V is the ejection velocity and V_e the escape velocity of Vesta. The hyperbolic eccentricity e is derived from the conservation of energy and can be expressed as follows as a function of V and V_e:

$$e^2 = 1 + 4\frac{V^2(V^2 - V_e^2)}{V_e^4}\sin^2(\alpha_0). \quad (9)$$

At infinity, when the fragment is outside the influence sphere of Vesta, the true anomaly is $f_\infty = \arccos(-1/e)$, so the deflection from the vertical at the ejection point (α_∞) is given by:

$$\alpha_\infty = f_\infty - f_0, \quad (10)$$

while the magnitude of the velocity becomes $V_\infty = (V^2 - V_e^2)^{1/2}$. Of course, the α_∞ angle is larger for those fragments whose ejection velocities are closer to the escape velocity. For instance, if $\alpha_0 = 45°$, α_∞ becomes 48°.4, 73°.0, and 88°.9 when V is equal to $2V_e$, $1.2V_e$ and $1.01V_e$, respectively. From the velocity distribution of the fragments and assuming for their starting position the position of the parent body, we can thus derive the orbital distribution of the simulated family members in proper element space.

4. Formation, size distribution and age of the family

In this section we study the collisional formation of the family and in particular we explore whether it may have been produced directly from a recent cratering event or if any post–formation collisional evolution is required to explain its observed properties. We use the collisional model described in Sect. 3 to predict the size and orbital element distribution of the family generated by a cratering impact on Vesta. Whenever we find model results consistent with the observations, we have a candidate scenario in which the family was formed in the recent past, i.e. it would be a "young" family. To estimate an upper limit for the family age, the post–formation collisional evolution process must be also modeled — providing at the same time a way to reconcile the model results with the observed family if the latter is not well represented by a "recent" cratering event.

In order to simulate the post–formation collisional evolution process, we are going to adopt the numerical algorithm developed for this purpose by Marzari et al. (1995). With a Monte Carlo method, they calculated the number of family members in any given size bin which would be involved in catastrophic collisional events within a given timestep ($\sim$ 1 Myr). The average flux of asteroidal projectiles is evaluated according to the Galileo team population estimate (Belton et al. 1992), used to compute the cratering age of (951) Gaspra and (243) Ida (for the corresponding uncertainty, see Farinella & Davis 1994). The outcomes of all these fragmentation events, in particular the size and orbital distributions of the resulting fragments, are calculated from a semi–empirical model similar to those of Davis et al. (1989) and Petit & Farinella (1993). At the end of each timestep, the overall size and orbital distribution of the family is updated taking into account the results of each single collision. In this way, the evolution of the size and orbital distribution of the family is followed in time. The collisional erosion process affecting the family is particularly effective at small sizes, where the depletion rate of the family members due to subsequent collisions is faster with respect to the large, more resistant, bodies. The global effect of this erosion process is to induce a progressive decrease of the characteristic exponent of the size distribution (the slope in a log–log plot of the cumulative number of family members vs. diameter).

Some other details on the collisional model are the following. The collision rate (specified by an intrinsic collision probability $P_i = 2.91 \times 10^{-18}$ km^{-2} yr^{-}1) and the average impact velocity (5.3 km/s) are taken from Farinella & Davis (1992). The smallest logarithmic size bin for the family asteroids considered in the simulation is centered at a diameter of 1.8 km. The Housen et al. (1991) strain–rate scaling law, including gravitational self–compression effects [Eq. 2 in Davis et al. 1994, with $k \approx 100$], is adopted for computing the impact strength S, namely the amount of projectile energy per unit of target volume needed to barely shatter the target itself. The resulting value for S is about 10^7 erg/cm^3 in the size range 1–10 km, hence the smallest projectiles which can shatter the family members included in the model (and therefore have to be taken into account in the simulations) are about 100 m across. The inelasticity coefficient f_{KE}, required to compute fragment speeds, is assumed to be 0.16, consistent with the observed dispersion in proper element space of the main asteroid families (Davis et al. 1989, Marzari et al. 1995).

First, we apply our collisional model to find out whether some particular cratering event can provide a good fit to the observed size distribution of the family, without any further collisional evolution. In Fig. 5 we show in the same frame three simulated size distributions, obtained with the three different approaches PF93, VBC and M89 (see Sect. 3), compared with the observed distribution. With the PF93 approach, we reach a

© European Southern Observatory • Provided by the NASA Astrophysics Data System

1996A&A...316..248M

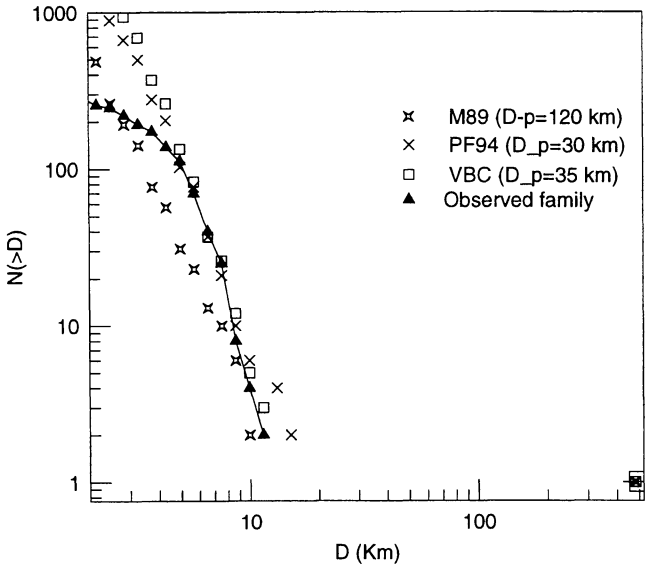

Fig. 5. Simulated cumulative size distributions of the Vesta family obtained with three different approaches for predicting the outcomes of large–scale cratering events (PF93, M89 and VBC; see text, Sect. 3), compared with the real size distribution of the family. Asteroid sizes are taken from the IRAS data base (Tedesco 1994) or calculated assuming an albedo value of 0.3. Note that the observed family is probably "complete" (i.e., all the existing members have already been discovered) only for diameters larger than about 5 km, causing an artificial decrease of the slope of the corresponding size distribution for smaller sizes.

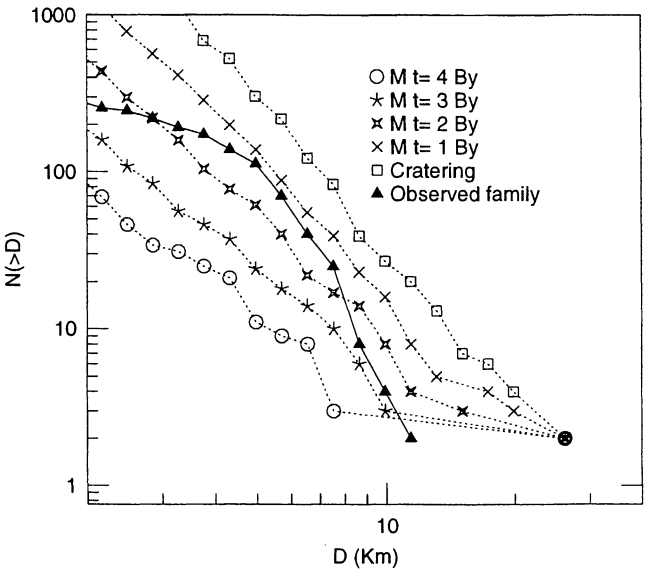

Fig. 6. The cumulative size distribution of a Vesta model family (generated with the PF93 approach) shown at different evolutionary times. The simulated impact is too energetic and the model family can never match the observed size distribution.

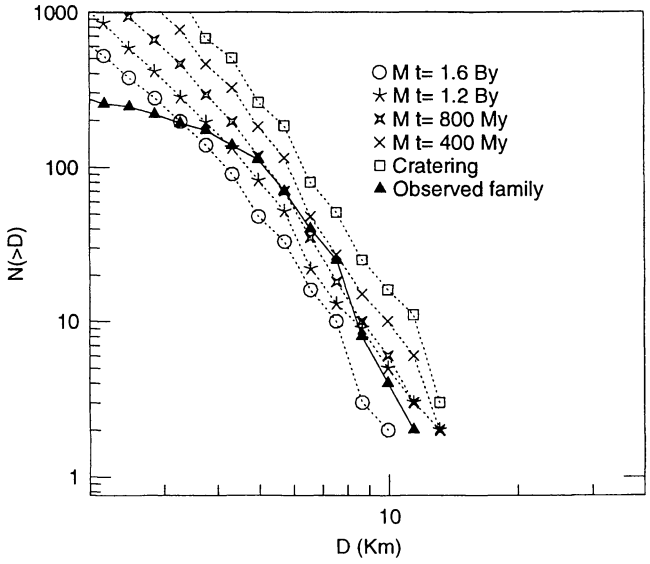

Fig. 7. The evolving size distribution for the transition model family obtained with the VBC approach (see text). After about 800 Myr since the initial cratering event a good match between the model and the real family is observed.

good agreement between the real and model distributions if we assume that the crater was generated by a projectile about 30 km in diameter. The excavated mass, according to Eq. 2, is about 1.5×10^{18} kg and the crater formed on the surface of Vesta has a diameter of about 250 km. The largest fragment produced by the impact has a diameter of 61 km and is reaccumulated, because its ejection velocity is lower than Vesta's escape velocity. The largest escaping fragment is a body $\approx$ 15 km in diameter, close to the size of the largest observed members in the family. Although the match to the observed family (and to the features observed on Vesta's surface, as summarized in Sect. 1) is good, one can question the physical plausibility of producing large fragments of a diameter that exceeds both the probable thickness of Vesta's crust, and the depth of the crater. The fact that all such large fragments are reaccumulated does not solve the problem.

From this point of view, the VBC approach is more satisfactory. Results similar to those reported above for PF93 are obtained in this case using a slightly larger projectile (35 km in diameter) and the same values for all the other parameters. In this case most of the largest fragments (25 km in diameter) are again reaccumulated, and the escaping ones reach about 12 km. Like for PF93, the model family is much richer than the observed one in small bodies (diameter less than $\approx$ 5 km), but this is easily explained by observational selection.

A very different scenario is obtained if we adopt the M89 approach. According to Eq. 4, a projectile 120 km in diameter is required to produce a largest fragment of about the same size as the observed largest family member, with the excavated mass amounting to about 18% of Vesta's mass according to the scaling equations of Holsapple (1993). Such an impact would either exceed the fragmentation threshold or get very close to it, depending on the adopted value of the impact velocity and of Vesta's impact strength (see Table 2 in Davis et al. 1994). An even more extreme conclusion was reached by Binzel & Xu (1993), who used similar scaling relationships for spall frag-

© European Southern Observatory • Provided by the NASA Astrophysics Data System

1996A&A...316..248M

ments to infer a projectile diameter in the range from 130 to 300 km. Although Vesta's self–gravity would allow it to survive an impact by a projectile up to about 250 km in diameter, such collisions appear unlikely to leave Vesta's basaltic crust (nearly) intact, and would rather fracture in depth the interior of the asteroid, or even convert it into a reaccumulated "pile of rubble" (Davis et al. 1979, Farinella et al. 1982). Another problem with this scenario is the fairly low probability of such a large impact having actually occurred on Vesta, $\approx 20\%$ over the whole age of the solar system — whereas impacts by ≈ 30 km projectiles are about an order of magnitude more frequent, i.e. a few such collisions are expected to have occurred over the solar system's lifetime (Davis et al. 1994). Finally, Fig. 5 shows that the family's size distribution predicted by the M89 approach does not really match the observed one, in particular in the size range between 5 and 8 km, where most observed family members are located. As a consequence, we consider more realistic the PF93 and VBC simulations than the M89 one, and in the following we will base our discussion on these scenarios, which, as we have seen, are fairly similar to each other as far as the projectile's size and the predicted size distribution of the family are concerned.

If within the PF93 and VBC approaches we increase the mass of the projectile or the impact speed, the cratering event becomes more energetic and the collisional outcome different. Since more energy is available to the ejecta, larger fragments can escape from Vesta and the model size distribution differs from the observed one both in slope and in absolute value. Hence, a evolution in time of the family is required in these cases to match the observations. The subsequent erosion of the family due to collisions with the asteroidal background population can in fact drive the model size distribution close to the real one at later evolutionary times. In this way, for a given cratering event we can estimate the age of the family, which coincides with the time required by the collisional erosion process to lower the size distribution of the family down to the observed one. Unfortunately, this does not lead to a unique solution for the origin and age of the family, because different combinations of projectile masses, impact speeds and ages can produce a family which would fit the observed one at some evolutionary stage. Nevertheless, we can set an upper bound to the age of the family. There is a limit to the amount by which the initial and current size distributions can differ. This limit is set by the lowering rate of the slope of the size distribution. In Fig. 6 we show the collisional evolution of a family generated by the impact of a 40 km body on Vesta (the PF93 approach is used here). The impact is so energetic that fragments about 30 km in diameter are ejected from Vesta. The lifetime of these fragments is long compared to the collisional erosion rate of the small family members. As a consequence, the size distribution of the model family crosses the observed distribution before the large size end of the distribution is eroded. Thus, all the families generated by impacts more energetic than the one illustrated in Fig. 6 will never be consistent with the real family. With the VBC approach, the same behavior is observed. Even if the fragments cannot be larger in size than the Vesta crust thickness, when we increase the impact energy many large $\approx$ 20–km sized fragments can escape. Again the time required to collisionally erode all these bodies is too long compared to the rate of decrease of the size distribution slope.

This argument shows that a transition family exists, marking the boundary between families matching the observations after some post–formation collisional evolution and those never matching the real family. In Fig. 7 we show such a transition family, obtained within the VBC approach, and generated by the impact of a projectile 40 km in diameter (the VBC approach always requires somewhat larger projectiles with respect to PF93). This family fits the observed size distribution after about 800 Myr since the initial cratering event. The limiting age derived with the PF93 approach is shorter, because there is no limitation to the size of the large fragments, as in the VBC approach. On this basis, we conclude that 1 Gyr represents an approximate upper bound to the age of the family. As we mentioned earlier (see also Davis et al. 1994, Farinella 1994), a projectile ≈ 40 km across and an age ≈ 1 Gyr for the Vesta family would be in reasonable agreement with the expected frequency of large–scale cratering impacts on Vesta.

5. Orbital distribution of the family

A preliminary analysis of the orbital distribution of the observed family in both the proper a–e and the proper a–i planes can help in putting some constraints on the angular orbital elements of Vesta at the time of the collision. To connect the variations in the proper orbital elements δa, δe and δi undergone by a given fragment (with respect to Vesta) with the components of its ejection velocity, we recall Gauss' equations (see Bertotti & Farinella 1990, Ch. 11) in the form given in Zappalà et al. (1990), namely with terms of order e^2 neglected:

$$\begin{aligned} 2\delta v_1/na &= \delta a/a \\ \delta v_2 sin(f)/na + 2\delta v_1 cos(f)/na &= \delta e, \\ \delta v_3 cos(\omega + f)/na &= \delta i \end{aligned} \tag{11}$$

where a, e, i, ω (perihelion argument), f (true anomaly) and n (mean motion) are the osculating orbital elements of the parent body when the collision occurs, while δv_1, δv_2 and δv_3 are the velocity components in the along–track, radial, and out–of–plane directions, respectively.

If we look at Figs. 2b and 4b, we see that in the observed family most of the fragments have higher inclinations with respect to Vesta. This means that for most of the crater ejecta the component δv_3 must be transformed into a positive variation of inclination, so $\cos(\omega + f)$ must be close to 1, i.e. $(\omega + f) \simeq 0$. We note also from Figs. 2a and 4a that the dispersion in e is not correlated with the dispersion in a. The first two Gauss' equations tell us that δe is independent of δa when $\cos f \simeq 0$, namely $f \simeq 90°$ (when on the contrary $f \simeq 0$, the maximum of correlation between δa and δe is obtained, and a family aligned along an oblique straight line in the a–e plane is generated). Since in our case $f \simeq 90°$, the constraint on the sum $(\omega + f)$ requires ω to be $\simeq 270°$.

© European Southern Observatory • Provided by the NASA Astrophysics Data System

1996A&A...316..248M

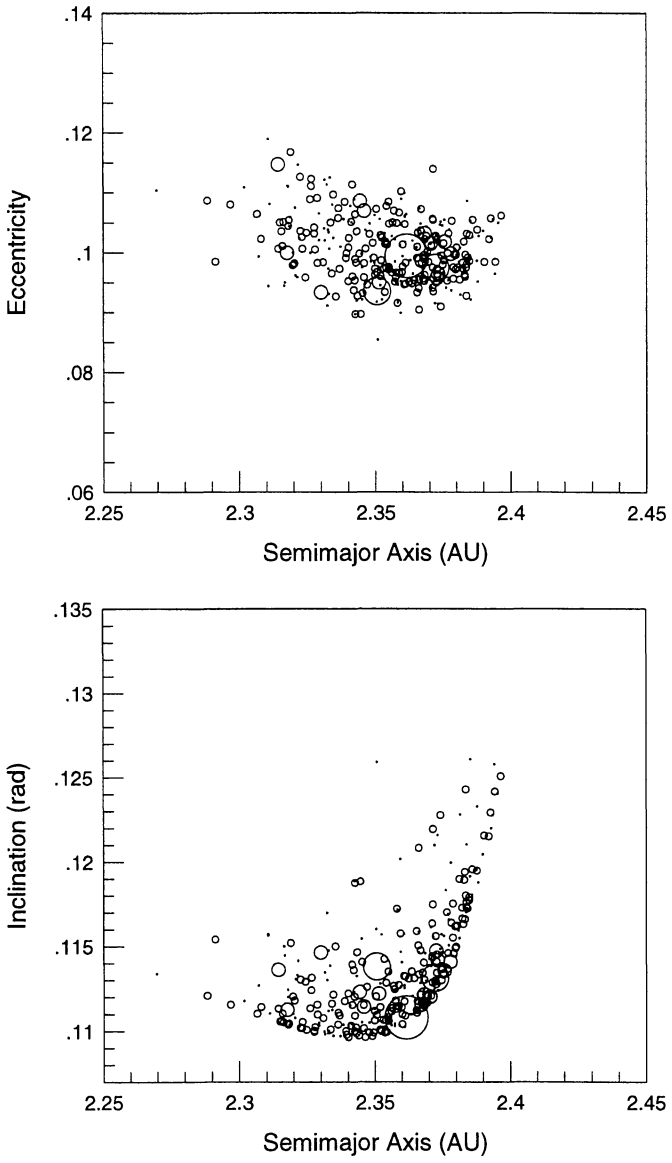

Fig. 8a and b. Model Vesta family, generated by the VBC approach and plotted in the proper a–e **a** and a–i **b** planes after 800 Myr since the original impact.

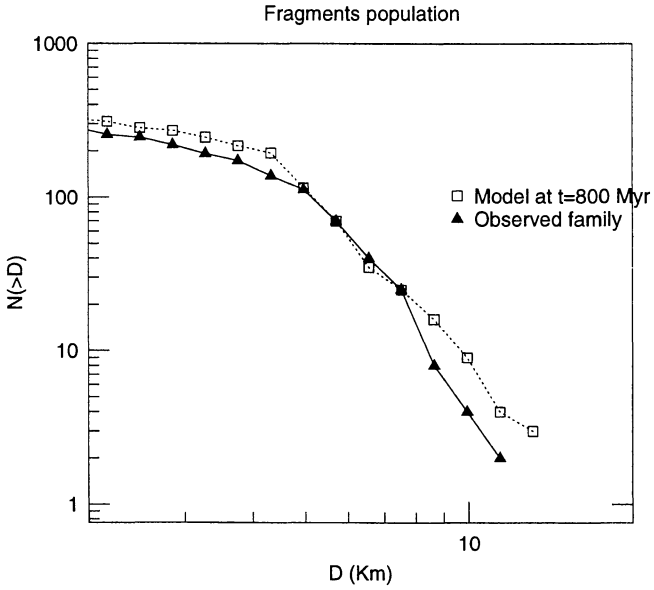

Fig. 9. Cumulative size distribution of the model Vesta family (VBC approach) after 800 Myr since the original cratering event. Different values for r and f_{KE}^{cr} have been used with respect to Fig. 7, in order to get a better match of the orbital distribution of the family, as discussed in the text.

Other two free parameters which are relevant in determining the shape of the family in proper element space are the two angles Θ and Φ which fix the direction of the axis of the ejecta cone in space. A first guess on their values can be made again looking at the proper element distribution in the real family. As we see from Figs. 2a and 4a, most of the fragments are located on the left side of Vesta in the a–e plane, suggesting that the impact occurred on the trailing hemisphere of the asteroid with respect to the direction of the orbital motion. On the other hand, the distribution in the a–i plane shown in Figs. 2b and 4b requires a positive value for Φ. To determine Θ and Φ, we have iteratively sampled values of these angles taking into account the above-mentioned constraints, until our model results have provided a reasonable match to the observed distribution of the family. Thus we have derived a possible set of angular parameters specifying the position of Vesta at the time of impact and the impact site on its surface: $f = 90°$, $\omega = 270°$, $\Theta = 170°$ and $\Phi = 40°$.

In Figs. 8a and b we show the orbital distribution of the model family obtained with the VBC approach after 800 Myr of post–formation collisional evolution (in agreement with the results reported in Sect. 4), to be compared with the corresponding morphology of the real family shown in Figs. 2a,b and 4a,b. To avoid the excessive clustering of small bodies in the model family plot (the power–law size distribution used by the model predicts in fact more than 3000 bodies between 1.8 and 5 km, the former being the lower cutoff adopted in our simulations), we have introduced an artificial selection effect. We randomly throw away family members in the model family at sizes smaller than the observational completeness limit, assumed to be around 5 km in diameter. The number of bodies left in the size bins below the completeness limit is equal to the number of observed family members of the same size.

We observe two main discrepancies between the model and and the real family: (1) the real family is considerably more dispersed both in the a–e and in the a–i plane; (2) the model family in the a–i plane has many members clustered near the edges of a parabolic structure (which is the counterpart of the conical geometry of the ejection velocity field), while the real family is more randomly distributed. Of course, there are at least two reasons why we should not expect a detailed match between the model and the real family: first, since the latter can be described as a "clan" (see Sect. 2), separating it in a sharp and unequivocal way from the random background is impossible; and second, although the proper elements have been shown by Milani & Knežević (1994) to be fairly stable over a time

© European Southern Observatory • Provided by the NASA Astrophysics Data System

1996A&A...316..248M

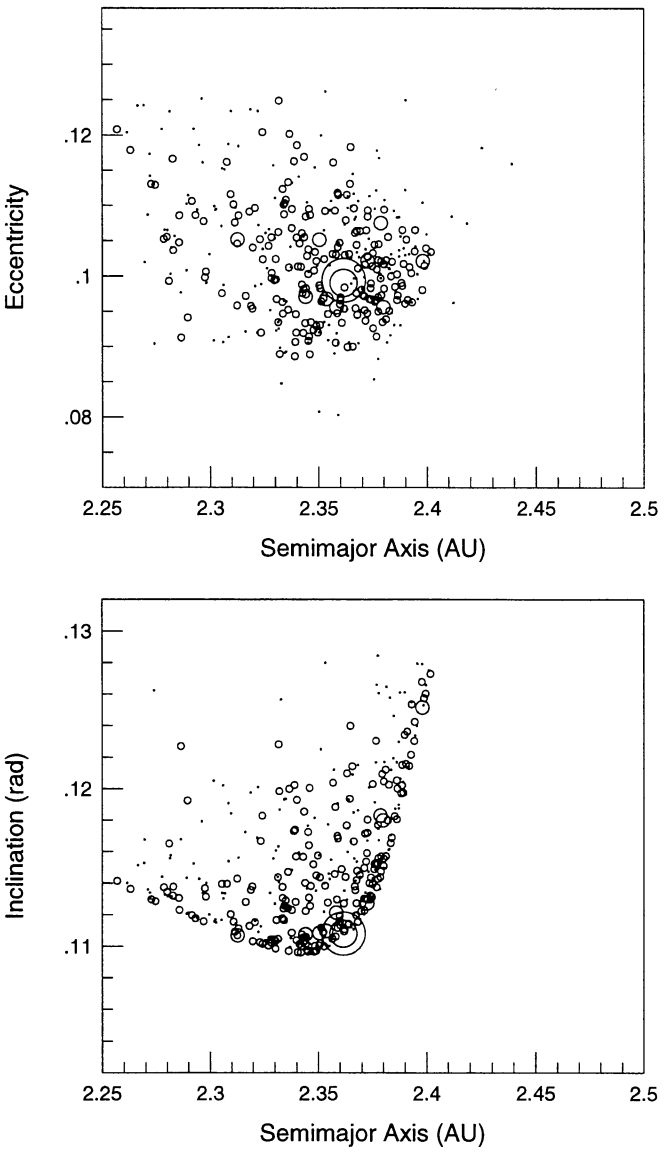

Fig. 10a and b. The same as Figs. 8, but with the alternative parameter choice for the fragment velocity vs. mass relationship used to derive Fig. 9 and discussed in the text.

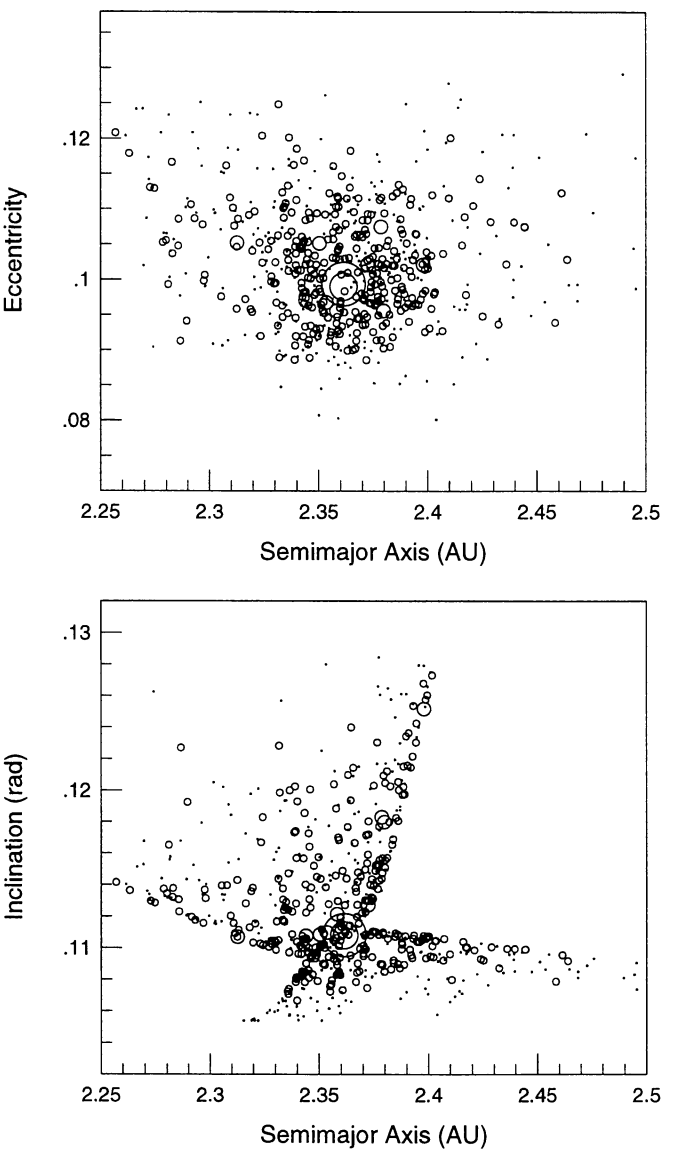

Fig. 11a and b. Orbital distribution in the proper a–e **a** and a–i **b** planes for a model Vesta family, generated in the double–impact scenario described in the text.

span of 5 Myr, the age of the family is probably some 200 times longer than this, and it is possible that subtle dynamical mechanisms have produced some "noise" in the proper eccentricities and inclinations, which may have partially masked the original distribution, preventing us from reconstructing its finer details.

While keeping these *caveats* in mind, however, we can look for possible modifications in our model which would improve the situation. The smaller dispersion in the orbital distribution of the model family can be ascribed to the way our model partitions the impact energy among the fragments. It is possible that the relationship between mass and velocity given by Eq. 5 does not hold over the entire mass range, but the ejection velocity for the smaller fragments, once reached a peak value, remains constant or even declines. If this is the case, when in our model we compute the coefficients r and V_0 from Eq. 6 and from the conservation of f_{KE}^{cr} times the impact energy, somewhat different values are derived. Thus, to obtain a better match between the model and real families, we have modified our model by increasing r to 0.25 [0.09 was the value predicted by Eq. 6] and assuming that 5 km/s (close to the propagation speed of the shock waves in the target) represents an upper bound for the ejection velocity of the small fragments. The size distribution of the family, shown in Fig. 9, is not significantly affected by this change if we adopt slightly different values for V_0 (80 m/s instead of 130 m/s) and, correspondingly, f_{KE}^{cr} (0.065 instead of 0.16). We stress that this alternative parameter choice is entirely within the range compatible with the experimental/observational results.

The orbital distribution of the model family shown in Figs. 10a and b presents a larger dispersion with respect to the previous model family and gives a better graphical overlap to the

© European Southern Observatory • Provided by the NASA Astrophysics Data System

1996A&A...316..248M

real family, except for the lower–inclination tail pointing toward the 3:1 Kirkwood gap. We have then assumed that this tail is the result of a second impact which occurred in the more recent past. Thus, we have combined into a single model family the fragments survived from a first impact occurred about 1 Gyr ago and those produced in a subsequent cratering event, for which we have assumed an age of just 200 Myr. A projectile 20 km in diameter has been selected for the second impact and different values for Vesta's orbital elements at the time of the impact and the coordinates of the impact site have been tested, with the same method outlined earlier in this section. The family obtained by merging the outcomes of the two impacts is shown in Figs. 11a and b. This is a plausible scenario for the formation of the family because: (1) Gaffey's (1983, 1996) rotationally resolved spectroscopic observation of Vesta, summarized in Sect. 1, suggests that more than one large crater is present on its surface; and (2) impacts with projectiles some 20 km across should occur on Vesta every 0.5–1 Gyr, according to the current estimates on the main belt population.

Comparing Fig. 11b with Figs. 2b and 4b, we are still disturbed by the clustering of bodies along the edges of the parabolic structures apparent in the model family in the a–i plane, whereas in the real family the distribution is much more randomly scattered within the same region. Although some "dynamical noise" on the proper elements could be responsible for the discrepancy, as discussed above, another explanation is possible. It is clear that the peculiar morphology of the model family in the a–i plane is the outcome of the somewhat artificial geometry of our ejecta model, according to which all the fragments are ejected on a conical surface. Although laboratory experiments show that this is a good approximation for cratering impacts into plane surfaces, this geometry results into a well-defined a–i distribution, with most of the fragments concentrated near the parabolic curve which limits the region populated by the family members. To obtain a better agreement with the observed orbital distribution, we have tested a different ejection geometry, assuming that (1) the opening angle of the ejection cone with respect to asteroid's center is 90°, as a result of the surface's curvature (see Sect. 3); and (2) the velocity vectors of the fragments are isotropically distributed *within* the cone (actually, an entire hemispheric region) whose axis is perpendicular to the surface at the impact site. Although these assumptions are somewhat *ad hoc*, we stress that little is known on the ejecta from impacts generating craters of size comparable to that of the target body, and therefore we felt that exploring different assumptions on this issue was justified. In Figs. 12a and b we show the model family generated with a single impact (like in Figs. 10) characterized by the modified ejection geometry. A more scattered distribution of the fragments in the a-i plane is produced, and some of the fragments are present the region between Vesta and the 3:1 resonance (the hyperbolic trajectory of the fragments plays a significant role here). A second impact is not necessary in this case to establish a link between the Vesta fragments and the resonance, because the subgrouping in the direction of the 3:1 resonance can be reproduced in this case.

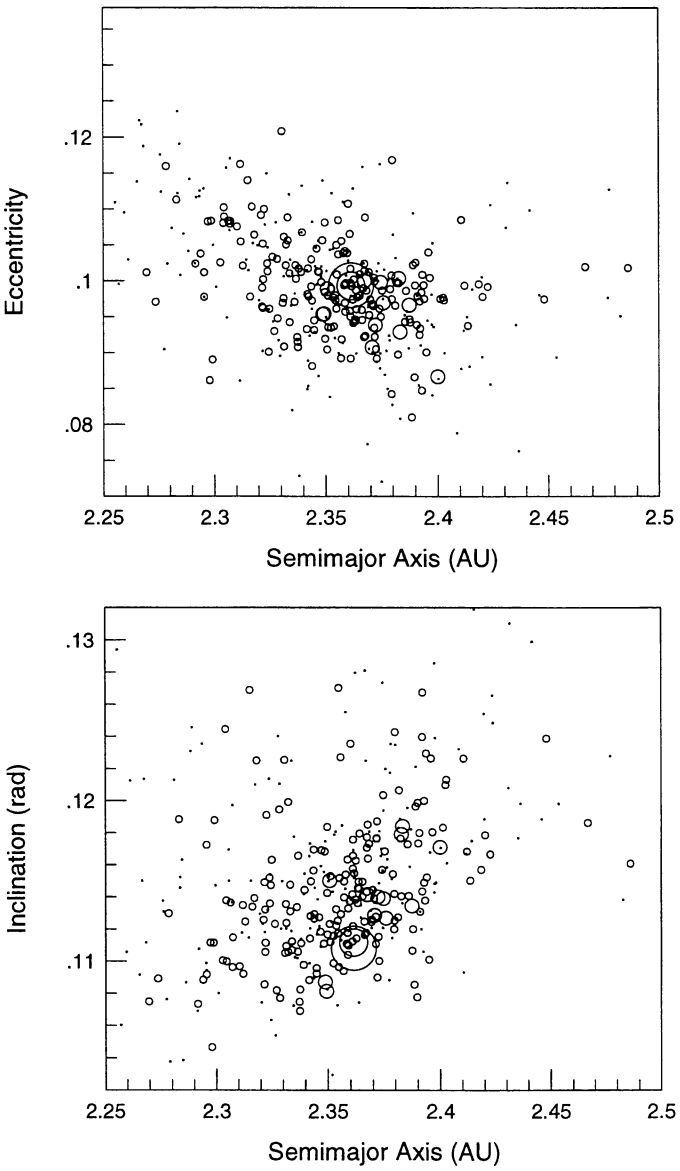

Fig. 12a and b. Single–impact model family with a modified fragment ejection geometry, as explained in the text.

The connection between the Vesta family and the 3:1 resonance can be made more manifest within our modeling, if we plot the family of Figs. 12 just after the breakup, without introducing the simulated observational selection effect. In Fig. 13 we show the model family produced by the simulated cratering event in the a–e plane, with all the members predicted by the power–law distribution for the fragments down to 1.8 km in diameter. The number of bodies injected into the 3:1 resonance is about 50, and some are as big as 4 km in diameter. On the other hand, the border of the ν_6 secular resonance is so far away from the location of the family (more than 1 km/s in terms of velocity increment, according to Farinella et al. 1993) that no sizeable fragment reaches this resonance.

© European Southern Observatory • Provided by the NASA Astrophysics Data System

1996A&A...316..248M

6. Discussion and conclusions

The purpose of this study was to understand what the properties of the present Vesta family can tell us about the age of family itself, the collisional history of Vesta and the physics of large–scale cratering events on asteroids. According to our numerical modeling, there are two possible scenarios for the formation of the Vesta family: (1) The formation of two large impact craters on the surface of Vesta, formed by projectiles $\approx$ 40 and 20 km in diameter hitting at different times in the past Gyr, with the merged ejecta from these two events forming the present Vesta family. (2) A single cratering event by a $\approx$ 40 km sized projectile, provided that a somewhat different ejection geometry of fragments with respect to that observed in small–scale laboratory experiments is assumed. In both cases an upper bound to the age of the family of about 1 Gyr is derived from the rate of the collisional erosion process for the small family members. These scenarios for the origin of the family are consistent with the telescopic observations of Vesta's surface (spectroscopy, photometry, polarimetry, speckle interferometry), which strongly suggest the existence of large impact basins on the basaltic crust of this asteroid.

An interesting aspect of our numerical approach is the computation of the orbital element distribution of the family at different evolutionary stages. Comparing the family distribution with the location of the 3:1 Jovian resonance, we can estimate how many fragments from the family–forming cratering event(s) could be injected into this resonance and then inserted into Earth–crossing orbits, becoming V–type near–Earth asteroids and HED meteorites. As shown in Fig. 13, several tens of fragments a few km in diameter (and many more smaller ones, according to the assumed power–law size distribution of the ejecta) were delivered to the 3:1 resonance. In other words, in its early stages the Vesta family extended enough in proper element space to reach (and overlap) the resonance. Later on, the collisional erosion process produced a shrinkage of the family, making the identification of the link with the resonance more difficult.

This conclusion is consistent with the recent results by Farinella et al. (1993), who have shown that with reasonable assumptions on the ejecta velocity distribution, some 2% of the fragments escaping from Vesta fall in the 3:1 resonance and may become Earth-crossers. As a consequence, Vesta's fragment delivery efficiency to Earth–crossing orbits accounts for 1% to 6% of the total from the asteroid belt, a fraction in reasonable agreement with the current observed abundance of HED meteorite falls (see e.g. Sears & Dodd 1988).

Also, three V–type NEAs have been identified by Cruikshank et al. (1991), two with diameters $\approx$ 3 km and one with a $\approx$ 1 km diameter; since their H magnitude is about 15, we may expect that some additional similar, undiscovered bodies exist [actually, Wisniewski (1991) suggested that also the small Apollo object (3361) Orpheus is probably a V type]. An intriguing hypothesis is that these bodies may have been generated by the (or one of the) event(s) that formed the family. Since the dynamical transport time through the 3:1 resonant *route* to Earth–

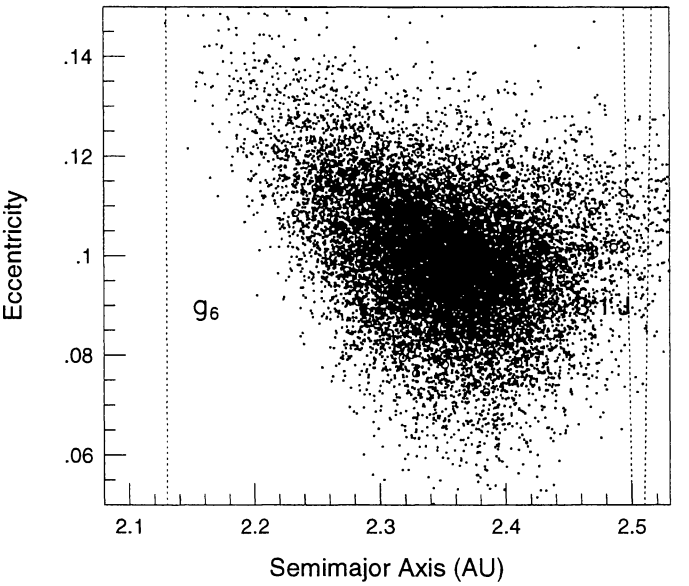

Fig. 13. The model Vesta family of Figs. 12 just after the impact. All the family members predicted by the power law for the ejecta size distribution down to 1.8 km diameter are plotted. The edges of the 3:1 resonance have been drawn based on the results of numerical experiments by Wisdom (1983, 1985) and Yoshikawa (1990), whereas the position of the edge of the ν_6 (or $g = g_6$) secular resonance has been located according to results by Kneževic et al. (1991).

crossing orbits is of the order of 1 Myr (Farinella et al. 1994, Moons & Morbidelli 1995) and, once in the Earth–crossing state, the lifetime of NEAs/meteorites vs. impacts against the inner planets is of the order of 100 Myr (Bottke et al. 1994), either these bodies have been formed in the most recent of the family–forming cratering events (e.g. in the double–impact scenario described in Sect. 5), or they just represent the surviving "tail" of an originally much larger population of NEAs coming from Vesta.

Concerning the HED meteorites, some information on their history is provided by laboratory studies. In our opinion, the available data do not allow one to link them directly to the family–forming event(s). For instance, cosmic–ray exposure ages of eucrites range from about 5 Myr up to 80 Myr (Euster & Michel 1995). However, the latter value is only a lower bound to the age of the original collisional event ejecting the meteorites from their parent body, because the cosmic–ray exposure clocks start when the samples are covered by less than about one meter of material, and thus, usually, when the original fragments have been reduced to meter–sized bodies. Such objects have probably collisional lifetimes on the order of 10 Myr, and therefore it is likely that the vast majority of the stony meteorites are just multi–generational fragments, formed from a sequence of impacts undergone while *en route* to the Earth.

The typical dynamical transport times and collisional lifetimes quoted above imply that HED meteorites begin to strike the Earth $\approx$ 1 Myr after their ejection from Vesta, and that the subsequent impact flux decreases exponentially with a characteristic decay time of $\approx$ 10–100 Myr. Thus, the current Earth in-

© European Southern Observatory • Provided by the NASA Astrophysics Data System

1996A&A...316..248M

flux from the original family–forming event(s) should be small, and most HED meteorites should originate from more recent, smaller impacts on Vesta (or other family members).

Other types of data provide some further constraints. Whereas the crystallization times of HED meteorites are $\approx$ 4.45–4.55 Gyr, Bogard & Garrison (1989, 1993) reported that ^{39}Ar–^{40}Ar analyses of individual clasts from these meteorites show reset ages across a wide span of time, mostly between about 3.4 and 4.2 Byr ago (there are some exceptions, however: one diogenite age is 1.1 Gyr). According to these authors, these ages reflect a number of distinct impact heating/melting events which possibly occurred during a prolonged early bombardment phase in the history of the inner solar system. Unless our upper limit of $\approx$ 1 Gyr on the age of the Vesta family is grossly wrong (and this might only be due to a strong overestimation of the projectile flux or to an underestimation of the impact strength for the minor family members), the age–resetting events are much older than the family–generating impact(s). Why have the latter impact(s) not been recorded in a more obvious way in the meteorites?

The answer is probably complex. First, the extent of isotopic resetting decreases with decreasing crater size and the amount of melt generated, and it is reasonable to assume that the older events — possibly occurred at a time when the projectile flux in the asteroid belt was significantly higher than now — were much more energetic than the later ones (perhaps they were close to the threshold for catastrophic break–up of Vesta, namely involved projectiles $\approx$ 100 km in diameter — see Table 2 in Davis et al. 1994). Subsequently, the associated families may have been eroded away and/or overlapped by the ejecta from more recent (though less energetic) collision(s). The meteorites could record only (or mainly) the older events because the most recent ones were not effective enough in resetting Ar–Ar ages of ejecta, and/or because they were ejected by smaller–scale impacts occurred on parts of Vesta's surface unaffected by the family–forming impact(s). Also, we may have a biased sample of the material generated in the family–forming event(s): in general, there is an unexplained paucity of impact melt material in meteorites (D. Kring, personal communication), and the same filter may have prevented shock–degassed samples of the family–forming event(s) from reaching Earth.

In comparing the orbital distribution of the real family (Figs. 2a,b and 4a,b) with the model family (Figs. 12a,b), we still observe some discrepancies which lead us to think that the real history of the Vesta family may have been more complex than our simplified model allows for. Possibly a sequence of more than two cratering events was involved, or some sizeable first–generation fragments were subsequently disrupted and generated subgroupings in the family. Adding to this, the stability of the proper elements over times of the order of 10^9 yr is far from guaranteed, since on such long time spans slow, diffusion–like phenomena have been evidenced in proper element space in other regions of the asteroid belt (Milani & Farinella 1994). Finally, the adjustments to the mass–velocity distribution and the geometry of the ejection velocity field which are required to better reproduce the real family suggest that it is not a straightforward task to scale up the laboratory results in order to describe the outcomes of real impacts between asteroids.

We have addressed here some problems which we have encountered in interpreting the Vesta family in terms of the present knowledge of cratering physics and ejecta dynamics. More experiments, theoretical models and empirical data on large–scale impacts on celestial bodies (including the Moon and the Earth) are necessary to provide a more complete understanding of the events which occurred during the formation and the subsequent history of the Vesta family.

Acknowledgements. We are grateful to H. Haack and D. Kring for several useful comments on an earlier version of this paper. This work has been partially supported by the Italian Space Agency (ASI) and by the Italian Ministry for University and Scientific Research (MURST). This is PSI contribution no. 331.

References

Belton M.J.S., Veverka J., Thomas P., Helfenstein P., Simonelli D., Chapman C., Davies M.E., Greeley R., Greenberg R., Head J., Murchie S., Klaasen K., Johnson T.V., McEwen A., Morrison D., Neukum G., Fanale F., Anger C., Carr M., Pilcher C., 1992, Science 257, 1647.

Bendjoya Ph., 1993, A&A Suppl. Ser. 102, 25

Bendjoya Ph., Slezak, E., Froeschlé, C., 1991, A&A 251, 312

Bendjoya Ph., Cellino A., Froeschlé C., Zappalà V., 1993, A&A 272, 651

Bertotti B., Farinella P., 1990, Physics of the Earth and the Solar System, Kluwer, Dordrecht

Binzel R. P., Xu S., 1993, Science 260, 186

Bogard D.D., Garrison D.H., 1989, Lunar Planet. Sci. XX, 90

Bogard D.D., Garrison D.H., 1993, Meteoritics 28, 325

Bottke W.F., Nolan M.C., Greenberg R., Kolvoord R.A. 1994, in Hazards Due to Comets and Asteroids (T. Gehrels, ed.), pp. 337–357, Univ. of Arizona Press, Tucson

Broglia P., Manara A., 1989, A&A 214, 389

Cellino A., Zappalà V., 1993, Celest. Mech. 57, 37

Cellino A., Zappalà V., Di Martino M., Farinella P., Paolicchi P., 1987, Icarus 70, 546

Cellino A., Di Martino M., Drummond J., Farinella P., Paolicchi P., Zappalà V., 1989, A&A 219, 320

Cruikshank D.P., Tholen D.J., Hartmann W.K., Bell J.F., Brown R.H., 1991. Icarus 89, 1

Davis D.R., Chapman C.R., Greenberg R., Harris A.W., 1979, In Asteroids (T. Gehrels, ed.), pp. 528–557, Univ. of Arizona Press, Tucson

Davis D.R., Chapman C.R., Weidenschilling S.J., Greenberg R., 1985, Icarus 62, 30

Davis D.R., Farinella P., Paolicchi P., Weidenschilling S.J., Binzel R.P., 1989, in Asteroids II (R.P. Binzel, T. Gehrels, & M.S. Matthews, eds.), pp. 805–826, Univ. of Arizona Press, Tucson

Davis D.R., Ryan E.V., Farinella P., 1994, Planet. Space Sci. 42, 599

Drake M.J., 1979, in Asteroids (T. Gehrels, ed.), pp. 765–782, Univ. of Arizona Press, Tucson

Drummond J., Eckart A., Hege E.K., 1988, Icarus 73, 1

Dunham D.W., 1991, Occultation Newsl. V, 93

Eugster O., Michel Th., 1995, Cosmochim. Geochim. Acta 59, 177

Farinella P., 1994, in Seventy–Five Years of Hirayama Asteroid Families: The Role of Collisions in the Solar System History (Y. Kozai, R.P. Binzel & T. Hirayama, eds.), Astron. Soc. Pac. Conf. Ser. 63, 76

© European Southern Observatory • Provided by the NASA Astrophysics Data System

1996A&A...316..248M

Farinella P., Davis D.R., 1992, Icarus 97, 111
Farinella P., Davis D.R., 1994, Lunar and Planet. Sci. XXV, 365
Farinella P., Paolicchi P., Zappalà V., 1982, Icarus 52, 409
Farinella P., Davis D.R., Cellino A., Zappalà V., 1992, in Asteroids, Comets, Meteors 1991 (A. Harris & E. Bowell, eds.), pp. 165–166, Lunar and Planetary Institute, Houston.
Farinella P., Gonczi R., Froeschlé Ch., Froeschlé C., 1993, Icarus 101, 174
Farinella P., Froeschlé Ch., Froeschlé C., Gonczi R., Hahn G., Morbidelli A., Valsecchi G.B., 1994, Nature 371, 314
Gaffey M.J., 1983, Lunar Planet. Sci. XIV, 231
Gaffey M.J., 1996, submitted to Icarus
Gaffey M.J., Bell J.F., Brown R.H., Burbine T.H., Piatek J.L., Reed K.L., Chaky D.A., 1994, Icarus 106, 573
Gault D.E., Shoemaker E.M., Moore H.J., 1963, NASA Tech. Note D–1767
Gratz A.J., Nellis W.J., Hinsey N.A., 1993, Nature 363, 522
Greenberg R., Chapman C.R., 1983, Icarus 55, 455
Greenberg R., Wacker J.F., Hartmann W.K., Chapman C.R., 1978, Icarus 35, 1
Knežević Z., Milani A., Farinella P., Froeschlè Ch., Froeschlè C., 1991, Icarus 93, 316
Holsapple K.A., 1993, Ann. Rev. Earth Planet. Sci. 21, 333
Housen K.R., Schmidt R.M., Holsapple K.A., 1991, Icarus 94, 180
Lupishko D.F., Belskaya I.N., Kvaratskhelia O.I., Kiselev N.N., Morozhenko A.V., Shakhovskoy N.M., 1988, Soviet Astron. Vestrik 22, 142
Marzari F., Davis D.R., Vanzani V., 1995, Icarus 113, 168
McCord T.B., Adams J.B., Johnson T.V., 1970, Science 168, 1445
Melosh H.J., 1989, Impact Cratering, Oxford University Press, New York
Migliorini F., Zappalà V., Vio R., Cellino A., 1995, Icarus 118, 271
Milani A., Farinella P., 1994, Nature 370, 40
Milani A., Knežević Z., 1992, Icarus 98, 211
Milani A., Knežević Z., 1994, Icarus 107, 219
Milani A., Farinella P., Knežević Z., 1992, in Interrelations between Physics and Dynamics for Minor Bodies in the Solar System (D. Benest & C. Froeschlé, eds.), pp. 85–132, Editions Frontières, Gif–sur–Yvette
Milani A., Bowell E., Knežević Z., Lemaître A., Morbidelli A., Muinonen K., 1994, in Asteroids Comets Meteors 1993 (A. Milani, M. Di Martino & A. Cellino, eds.), pp. 467–470, Kluwer, Dordrecht
Moons M., Morbidelli A., 1995, Icarus 115, 60
Nakamura A., Fujiwara A., 1991, Icarus 92, 132
Nakamura A., Suguiyama K., Fujiwara A., 1992, Icarus 100, 127
Petit J.–M., Farinella P., 1993, Celest. Mech. 57, 1
Sears D.W.G., Dodd R.T., 1988, in Meteorites and the Early Solar System (J.F. Kerridge & M.S. Matthews, eds.), pp. 3–31, Univ. of Arizona Press, Tucson
Tedesco E.F., 1994, in Asteroids Comets Meteors 1993 (A. Milani, A. Cellino & M. Di Martino, eds.), pp. 463–466, Kluwer, Dordrecht
Tedesco E.F., Williams J.G. Matson D.L., Veeder G.J., Gradie J.C., Lebofsky L.A., 1989, in Asteroids II (R.P. Binzel, T. Gehrels, & M.S. Matthews, eds.), pp. 1151–1161, Univ. of Arizona Press, Tucson
Tholen D.J., 1989, in Asteroids II (R.P. Binzel, T. Gehrels, & M.S. Matthews, eds.), pp. 1139–1150, Univ. of Arizona Press, Tucson
Vickery A.M., 1986, Icarus 67, 224
Vickery A.M., 1987, Geophys. Res. Lett. 14, 726
Wetherill G.W., 1987, Phil. Trans. R. Soc. Lond. A 323, 323
Williams J.G., 1979, in Asteroids (T.Gehrels, ed.), pp. 1040–1063, Univ. of Arizona Press, Tucson
Williams J.G., 1989, in Asteroids II (R.P. Binzel, T. Gehrels, & M.S. Matthews, eds.), pp. 1034–1072, Univ. of Arizona Press, Tucson
Williams J.G., 1992, Icarus 96, 251
Wisdom J., 1983, Icarus 56, 51
Wisdom J., 1985, Nature 315, 731
Wisniewski W.Z., 1991, Icarus 90, 117
Yoshikawa M., 1990, Icarus 87, 78
Zappalà V., Cellino A., 1992, Celest. Mech. 54, 207
Zappalà V., Cellino A., 1994, in Asteroids, Comets, Meteors 1993 (A. Milani, M. Di Martino & A. Cellino, eds.), pp. 395–414, Kluwer, Dordrecht.
Zappalà V., Cellino A., Farinella P., Knežević Z., 1990, Astron. J. 100, 2030
Zappalà V., Cellino A., Farinella P., Milani A., 1994, Astron. J. 107, 772
Zappalà V., Bendjoya Ph., Cellino A., Farinella P., Froeschlé C., 1995, Icarus 116, 291
Zellner B., Storrs A., Wells E.N., 1995, Lunar Planet. Sci. XXVI, 1553

This article was processed by the author using Springer-Verlag LaTeX A&A style file *L-AA* version 3.

© European Southern Observatory • Provided by the NASA Astrophysics Data System